ISTITUTO NAZIONALE DI FISICA NUCLEARE

Sezione di Lecce

INFN/TC–95/13
15 Marzo 1995

A. Beloglazov, V. Nassisi, M. Primavera:

A STUDY OF PLASMA EFFECTS IN A "NON–PLASMA" REGIME IN ELECTRON BEAMS PRODUCTION ON Al TARGET BY EXCIMER LASER

PACS: 41.85.Ar; 42.62.ct; 52.50.-b

SIS–Pubblicazioni
dei Laboratori Nazionali di Frascati

INFN – Istituto Nazionale di Fisica Nucleare
Sezione di Lecce

INFN//TC–95/13
15 Marzo 1995

A STUDY OF PLASMA EFFECTS IN A "NON–PLASMA" REGIME IN ELECTRON BEAMS PRODUCTION ON Al TARGET BY EXCIMER LASER

A. Beloglazov[a], V. Nassisi, M. Primavera

University of Lecce, Department of Physics and I.N.F.N., Lecce 73100 Italy
[a)] On leave from Institute of General Physics, 38 Vavilov street, Moscow Russia

Abstract

Experiments on electron beams production by XeCl and KrCl excimer lasers on Al target were performed below the threshold intensities for plasma ignition. Direct experimental evidence of a plasma formation below the ignition threshold is given for the first time. Positive potentials of 0.36 and 0.75 V at distances down to about 2 mm from the grounded target on the laser spot region have been measured by a Langmuir–like probe, respectively illuminating the target with XeCl and KrCl lasers. From this result and in absence of cathode voltage, an accelerating electric field of about 375 kV/m was estimated on the target, while the highest positive charge density near the cathode was about 3.3 mC/m^3. The strong electric field induced by the plasma formation, which modified the acceleration conditions of the electron beam, seems to be the main responsible of the discrepancies between the experimental current values and the ones obtained by solving the Child–Langmuir equation.

1. Introduction

Recently, experiments using metal photocathodes irradiated by excimer lasers have been shown that they can provide electron beams of high brightness and low emittance, better than that generated by thermionic sources [1–4]. These features have been confirmed by detailed investigations of electron emissions from Al, Zn and Cu targets illuminated by XeCl (308 nm) and KrCl (222 nm) laser radiation [5].

However, discrepancies between the experimental values of the current involved and the theoretically predicted ones using metal photocathodes [5, 6] and ferroelectric cathodes [7, 8] have been observed by many authors. In their works a large excess of the experimental space charge dominated current density with respect to the calculated one was reported. For

short anode–cathode distance compared to the laser spot dimension, the current density values calculated by the Child–Langmuir law are much larger than the experimentally measured ones [9]. It should be stressed that in all these experiments, laser power density values were under plasma ignition threshold and the plasma formed on the cathode modified the propagation conditions for a space charge dominated electron beam. Experiments performed with ferroelectric cathodes have also demonstrated the generation of charged particles with non–zero initial kinetic energy of about 25 kV [10] and 5kV [7]. Some authors which worked with ferroelectric cathodes [8], since thay didn't observe currents in absence of accelerating voltage, considered the initial electron kinetic energy as zero and found the solution of the 1D–Poisson equation in order to justify the experimental results. The potential which results as a solution of Poisson equation had a maximum value of four order of magnitude larger than the typical applied anode–cathode potential.

In this work, the experimental results of the excess of the output current from an Al cathode irradiated by a XeCl and KrCl laser with respect to the expected values are reported together with the emittance values. Experimental evidence of the plasma generation during the laser action is demonstrated. The theoretical calculations of the output current and beam emittances were obtained by using the EGUN simulation code, which did not take into account this strong plasma effect. In order to correct for this effect, especially for beam spots smaller than the anode–cathode distance, we numerically solved the 1D–Poisson equation in the case of space charge dominated electron beam which have experimental emittance and are subjected to the plasma effect.

2. Experimental setup

An Al target was placed on a supporting rod in a chamber evacuated down to 10^{-6} Torr by a turbo–molecular pump. The rod was mounted with an isolator and a fast Rogowski coil to a chamber flange shown in Fig.1. In this way the system was enabled to supply a high voltage to the target and measure the total current emitted from cathode. Facing the target at a 105 mm distance, there was an array of small Faraday cups which acted as anode. and allowed to measure the beam emittances.

A HV power supplier fed the cathode (T) by a coaxial cable having a capacitance of 100 pF/m. This last characteristic allowed to the cable to be used as a buffer capacitor. The maximum accelerating voltage applied was 20 kV.

Two different excimer laser were utilized for irradiating the target, a XeCl, whose wavelength was 308 nm and a KrCl, whose wavelength was 222 nm: the laser photon energies corresponds at 4.02 eV and 5.6 eV, respectively for the reported lasers. These values are respectively lower and higher than the work function of the Al (4.2 eV)

The target was struck by the laser beam at about 70° angle of incidence. To avoid the anode–cathode short–circuit by plasma ignition, the Al target was mirror–polished with a grain size 1/4 μm or less and the laser energies were chosen less than the short–circuit threshold values.

A coaxial Langmuir–like probe having the tip (P) 1 mm in diameter and 0.2 mm long was connected to a 50 Ω coaxial cable by a 4.8 kΩ resistor (Ro). The probe was

mechanically fixed to a movable feedthrough and the whole device was placed instead of Faraday cups flange in the accelerating chamber, as shown in Fig. 2. The input impedance of the probe was enough large. Three strips (S), connecting the external probe conductor to the grounded target support, avoided to pick up stray signals.

The calibration of the probe was accomplished by a fast voltage pulser closed to a 50 Ω load resistance and coupled to the probe tip. Fig. 3 shows the input signal (upper trace) and the probe response (lower trace) during the calibration. Its time behavior is excellent, as can be seen in Fig. 3, where the time scale is 20 ns/div. The experimental attenuation value was 96.

During the experiments the laser spot on the cathode surface was dimensioned by a convergent lens.

The laser pulse energies were controlled by a joulemeter Gentec ED–500. The temporal shape of the laser pulse was detected by a fast Hamamatsu R1328U–02 photodiode which served as a triggering source in the experiments with the Langmuir probe. Two digitizing oscilloscopes, Tek 540 (1 GS/s) and Tek 620 (2 GS/s), recorded the current and laser waveforms.

3. Results and discussions

Firstly, we fixed the laser spot diameter on the target at 2 mm. Choosing the XeCl laser energy at 5.6 mJ we recorded the output current by the Rogowski coil and the Faraday cups. Fig. 4 shows the output current and the emittance as a function of the accelerating voltage. The emittance value, in the plane of incidence of electrons, was calculated by the following formula [11] $\varepsilon_0 = r\,\Delta\phi/\pi$, where r is the spot radius and $\Delta\phi$ is the electron beam divergence. Fixing the KrCl laser energy at 3.8 mJ, the output current was detected as a function of the voltage. The current and the emittance values are shown in Fig. 5. Nevertheless, the KrCl laser energy used was lower than the XeCl one, the photoemission current was higher as well as the space charge effects and as a consequence also the emittance values. The current behavior was determined mainly by photoemission of electrons with different contributions because of volume photoeffect and surface photoeffect [12].

It could also be seen that the current pulse was slightly elongated compared to the laser one due to the increasing of target temperature [1]. Current peculiarities due to the different lasers could be described in terms of Al work function (4.2 eV) and KrCl and XeCl laser photon energies (5.6 and 4.02 eV respectively), but the propagation conditions ought to be always independent on the electron source. In fact the simulation by EGUN code gives a maximum current of only 200 mA and an emittance of 75 π mm mrad at 20 kV of accelerating voltage under space charge dominated regime. Fig. 6 shows the electron trajectories and the equipotential surfaces obtained by the simulation. From the experimental data with KrCl, we observe that the beam was not limited in intensity as the accelerating voltage increased, and then the saturation conditions were not reached nevertheless the maximum current density was 30 A/cm^2.

As suggested in Ref. 6, we investigated the plasma formation by the Langmuir–like probe. During this measurements the cathode was grounded and the probe tip was moved

away from target. Then, the cathode potential was zero, but just 2 μm from it the signal recorded by the probe was about 0.38 and 0.75 V, respectively for XeCl and KrCl laser. Fig. 7 and 8 show the laser pulses (lower traces) and the probe pulses (upper traces) at 2 mm distance from the target by XeCl and KrCl laser illumination, respectively.

The maximum probe pulse was obtained with the KrCl laser as well as the output current extracted with this laser was higher than that obtained with the XeCl laser.

In this case we can estimate an electric field on the target surface nearly to 375 kV/m. Further measurements gave potential values always lower versus the distance from cathode. At about 3–4 mm from it, the potential became zero and its distribution was fitted as an exponential function having the decay constant x_o nearly to 1–1.2 mm. Neglecting the electric field transversal components we supposed a charge density like:

$$\rho_{p(x)} = 3.3\ 10^{-3}\ e^{-x/x_o}\ [C/m^3]$$

To solve the 1D–Poisson equation, it is necessary to modify it in order to counterbalance the absence of the other coordinates. In this case, because of the longer anode–cathode distance in comparison to the beam spot near the target and of the result obtained by the EGUN code simulation, the 1D–Poisson equation was modified in order to include the influence of the small radial beam dimension. This last increased due on beam divergence, as shown in Fig.4, and on the strong r-direction acceleration at which the more external electrons are subjected mainly near the cathode. Therefore, as far as the first case the beam radius must be increased as αx where α is the half beam divergence, while as far as the second case the radial position must be governed by the following equation: $dr = a_r t dt$ where a_r is the radial acceleration and t is the time. Approximating the a_r to $\rho_e(x\ r)/r^2$ and considering that the electron distribution ρ_e depends on electron x- and r-direction velocity where the x- velocity depends on $V^{1/2}$ and the x- position could depend on $V^{3/2}$[13], the r-position becomes proportional to $x^{1/3}$ Therefore, under the above considerations, the 1D–Poisson equation is

$$d^2 V/dx^2 = I\ k\ /\ (V^{1/2}\ \pi\ (Ro + \Delta\phi/2x + \beta x^{13})^2)\ \rho_p\ /\ \varepsilon_o\ e^{-x/x} \qquad 1)$$

where I is the total current, k is a constant, $(m/2e)^{1/2}/e_o$, equal to 190000 ($A^{-1}\ V^{3/2}$), Ro is the initial radius, $\Delta\phi/2$ is the half beam divergence and β is a correction factor due to the strong acceleration at which the external electrons are subjected. Fixing Ro = 0.001 m, $\Delta\phi/2 = 0.2$ and $\beta = 0.09\ m^{2/3}$, we integrated numerically the Eq.(1) with $\rho_p = 3.3\ mC/m^2$ and with $\rho_p = 0$ from $x = 0$ to $x = 105$ mm. The results are reported in the Table I:

Table I: Results of the integration of the Eq. (1).

I [mA]	ρ_p[mC/m^3]	V(105mm)[V]
1000	3.3	~ 21000
200	0	~ 19200

The voltage values found are very near to 20 kV which is the experimental one, therefore the plasma effect justifies the increasing of the output current. In fact, with $\rho_p = 0$ the voltage applied is reached with only 200 mA as pointed out by the EGUN computer simulation.

It is important to note that with different expressions of the $\beta x^{1/3}$ term, we obtained a current behavior very similar to that described above, i e. we found equal final potentials fixing the current at 1 A and ρ_p at 3.3 mCm^3 or the current at 0.2 A and the ρ_p at zero.

Further studies of the plasma influence were performed with a larger beam surface (90 mm^2) and with shorter anode–cathode distances. We performed studies with anode–cathode distances shorter and larger than the beam diameter, but they allow in any case to negligible the beam enlargement. The experimental set up is shown in Fig. 9. The laser energy used was 30 mJ at 222 nm. Fig. 10 shows the theoretical values and the experimental values for a anode–cathode distance of 2 mm, while Fig. 11 shows the theoretical values and the experimental values for a anode–cathode distance of 16 mm. The theoretical current values shown in these last figures were calculated by the Child–Langmuir law ($I[A] = 210\ 10^{-6} V^{3/2}/x^2$, where x is the distance measured in mm). The experimental values at short distance are lower that the Child–Langmuir ones and this behavior was extensively explained in Ref. 9. Instead, the experimental values at large anode–distance distances are higher that the Child–Langmuir ones. Even in this case we integrated numerically the Eq. (1) with I= 500 mA and with $\rho_p = 3.3\ mC/m^2$. At 16 mm distance the voltage obtained was 3.8 kV, while putting $\rho_p = 0$ the voltage obtained was about 7.9 kV as can be even seen in Fig. 11. A plot of the results (experimental and theoretical values) at x =10 mm is shown in Fig. 12. For this distance the plasma effects are compensated.

4. Conclusions

We can conclude that, under our conditions and below spark ignition threshold, a plasma is formed near the target. It consists of fast electrons which go away from the spot area firstly and relatively slow ions which stay near the target for about 50 ns and produced a strong electric field. The field acts upon electrons induced by the laser pulse and favors their extraction from the target. We may conclude that, in order to simulate electron currents under our experimental conditions, we should modify the Poisson equation and to solve it for a space charge dominated electron beam. The origin of the detected plasma should be the subject of a special investigation. We can suppose it to be due to adsorbed surface species and (or) residual roughness and microsharpness of the surface. Undoubtedly, the described effect should be taken into account when developing new electron sources based on excimer laser induced photoeffect on metal cathodes.

The maximum output current density was 30 A/cm^2 under a KrCl excimer laser illumination.

Acknowledgements

The authors would like to thank Dr. V. Stagno for the EGUN simulation.

References

[1] D.W. Feldman, S.C.Bender, B.E. Carlsten, J. Early, R.B. Feldmann, W. Joel, D. Johnson, A.H. Lumpkin, P.G. O'Shea, W.E. Stein, R.L. Sheffield, and L.M. Yuong, IEEE J. Quantum Electron. **QE–27**, 2636(1991)

[2] V. Nassisi, Nucl. Instr. and Meth. **A 340** (1994) 182–185.

[3] D. Charalambidis, E. Hontzopoulos, C.F. Fotakis, G. Farkas and C. Toth, J. Appl. Phys. **65**, (1989) 2843.

[4] A. Beloglazov, M. Castellano, M.S. Causo, V. Nassisi and P. Patteri, Proc. CLEO 94, Amsterdam, the Netherlands, IEEE Cat.Num. **94TH0614–8**, (1994) 147.

[5] A. Beloglazov, M. Martino, V. Nassisi, to be published

[6] Y. Kawamura, K. Toyoda, M. Kawai, J. Appl. Phys. **71**, 2507 (1992).

[7] E. Sampayan, G.J. Caporaso, C.L. Holmes, E.L.Lauer, D. Prosnitz, D.O. Trimble, G.A. Westenskow, Nucl. Instr. and Meth. **A 340**, 90 (1994)

[8] L. Schachter, J.D. Ivers, J.A. Nation, and G.S. Kerslick, J. Appl. Lett. **73**, 8097 (1993)

[9] M.S. Causo, M. Martino, V. Nassisi, Appl. Phys. **B 59**, 19 (1994).

[10] H. Riege, Nucl. Instr. and Meth. **A 340**, 81 (1994)

[11] W. Namkung and E.P. Chojnacki Rev. Sci. Instrum.57 341 (1986) A. Beloglazov, M. Martino, V. Nassisi and V. Stagno, Proc. EPAC'94, London, UK, 1994.

[12] Gy. Farkas, Z.Gy. Horvàth, Cs. Tòth, C.F. Fotakis and E. Hontzopoulos, J. Appl. Phys. **62**, 4545 (1987).

[13] It is very difficult to determinate the dependence of the potential V on x– position especially when the exact electron radial dimension is not known. By the Child–Langmuir law x is proportional to $V^{3/4}$. Because the radial dimension increases as the x – dimension increases, then we expect that the potential value increases less that $x^{4/3}$, therefore we try with V proportional to $x^{2/3}$.

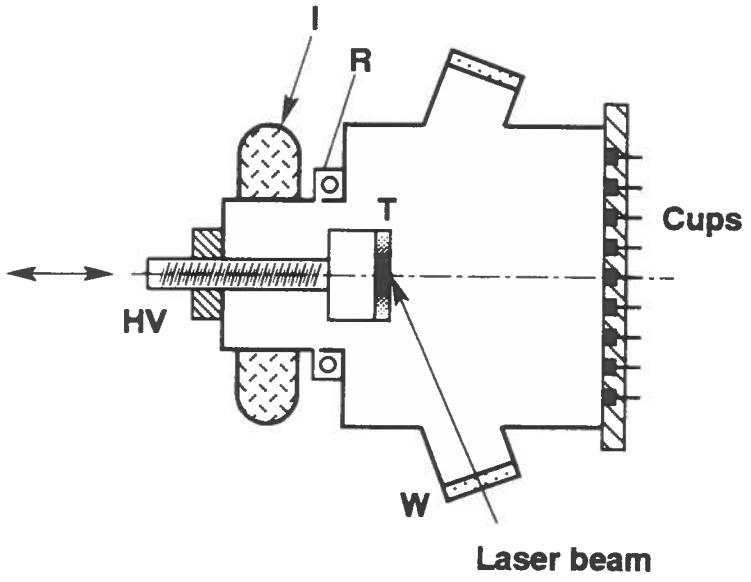

Fig. 1 – Accelerating chamber with Faraday cups. T; Target, I; Insulator, HV; high voltage, R; Rogowski coil and W; window.

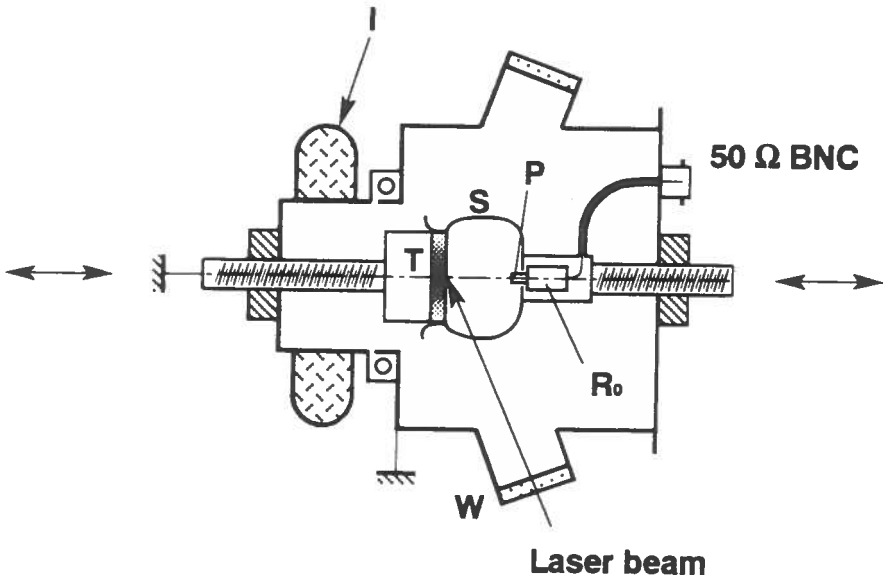

Fig. 2 – Accelerating chamber with Langmuir probe. T; Target, P; probe pin, Ro; 4.8 kΩ inner resistance, S; conducting strips, and W; window.

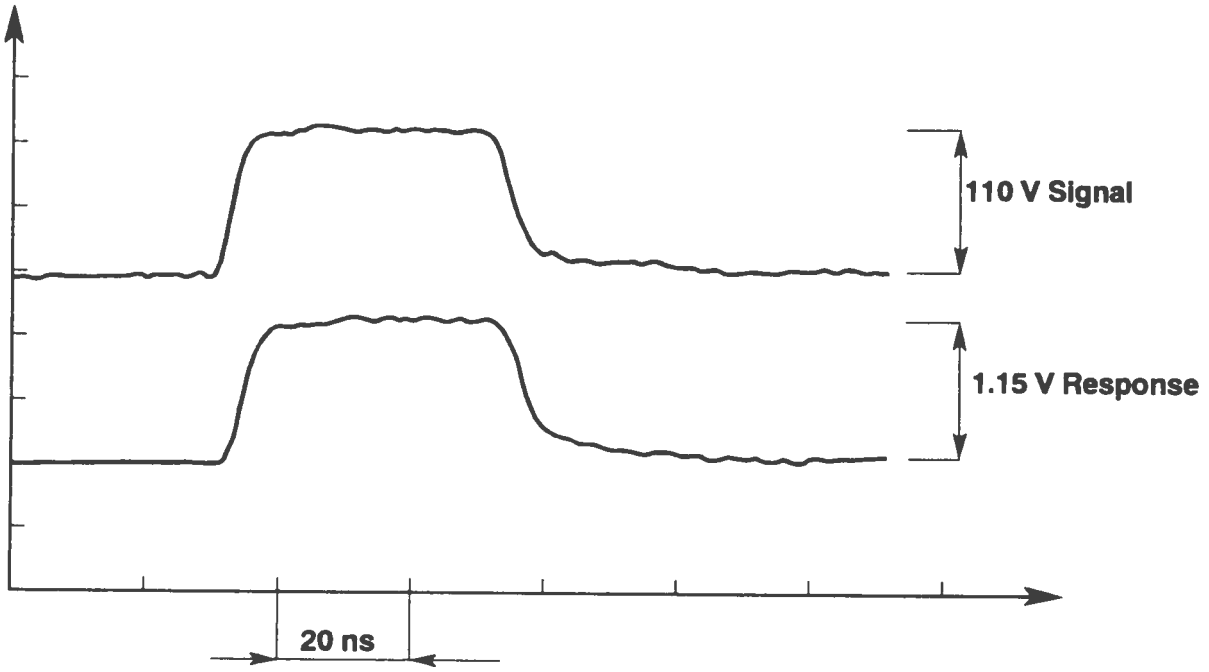

Fig. 3 – Calibration of the probe. Upper trace; signal applied to the probe pin, lower trace; response of the probe

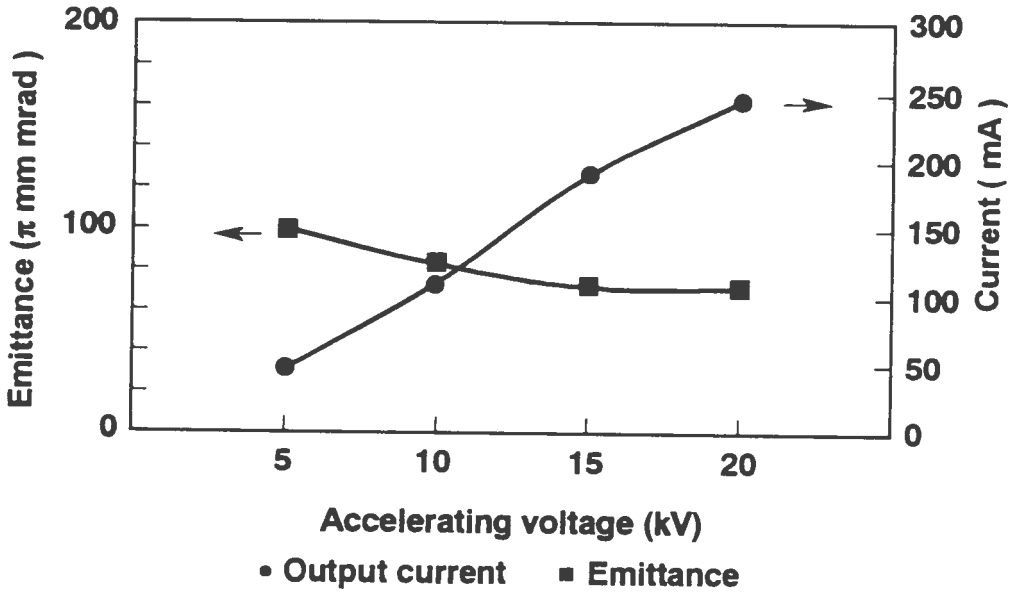

Fig. 4 – Current and emittance values of the photoextracted electrons from Al target vs. the accelerating voltage, the pulse energy was 5.6 mJ at 308 nm.

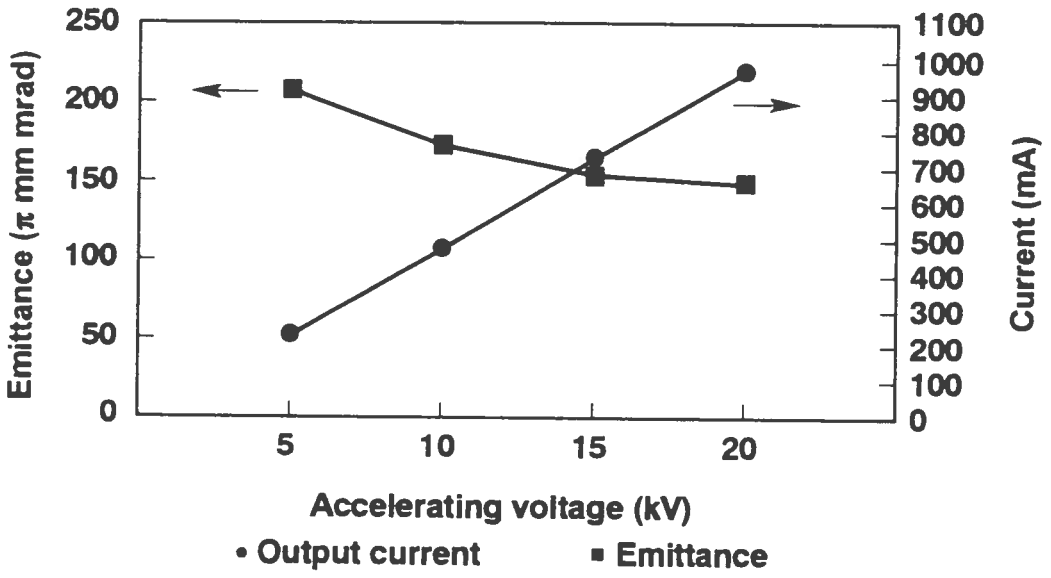

Fig. 5 – Current and emittance values of the photoextracted electrons from Al target vs. the accelerating voltage, the pulse energy was 3.8 mJ at 222 nm.

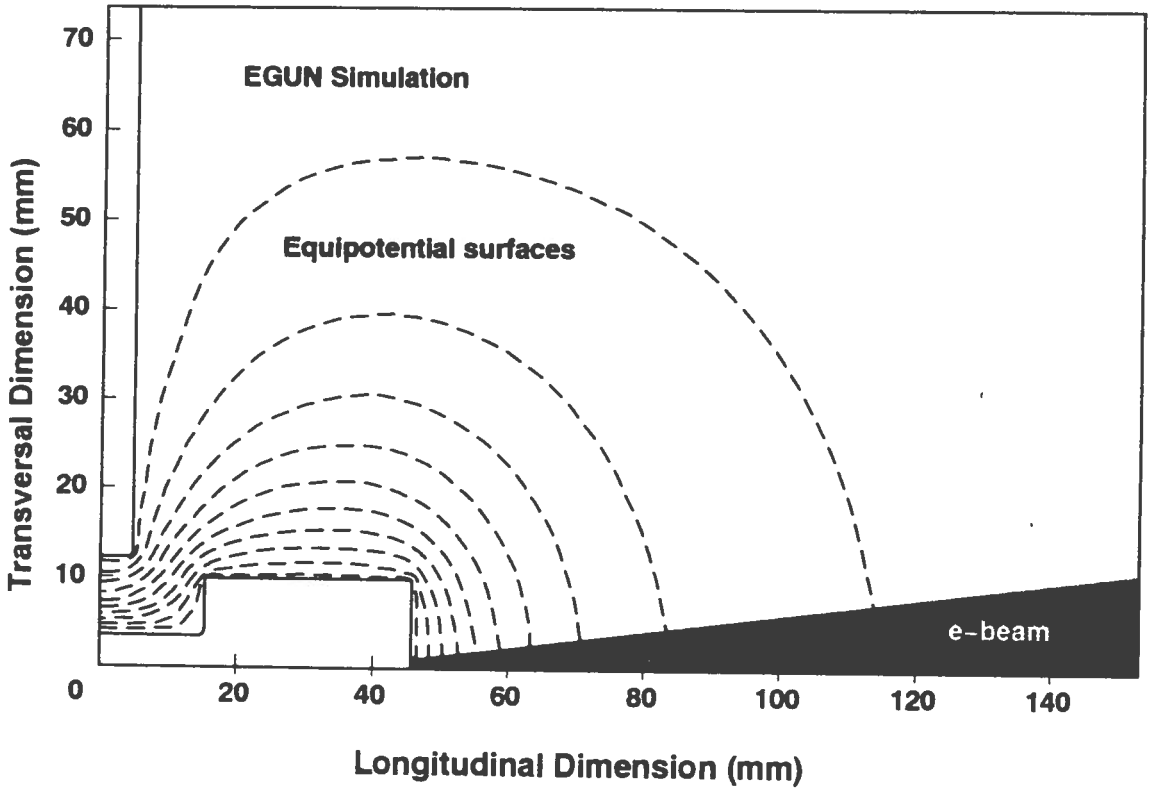

Fig. 6 – Electron trajectories and equipotential surfaces computed by EGUN simulation code.

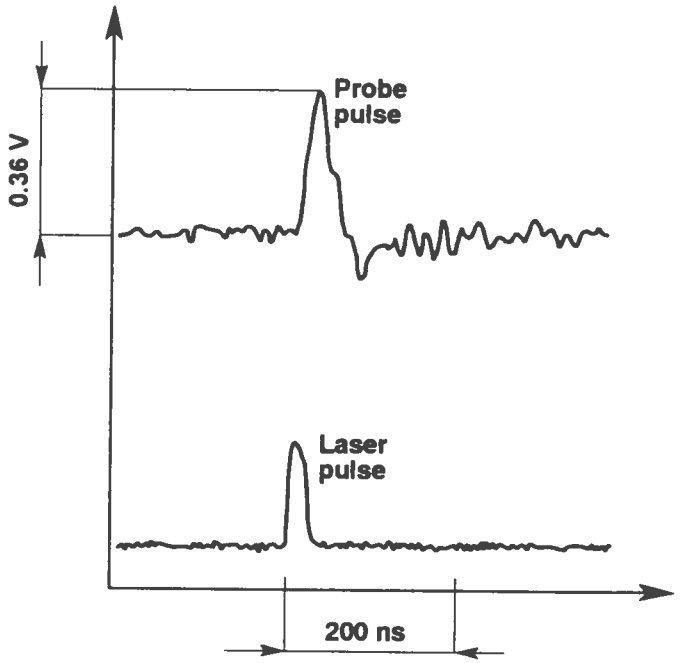

Fig. 7 – Waveforms of the XeCl laser pulse and of the Langmuir probe pulse. This last was recorded at 2μm from cathode.

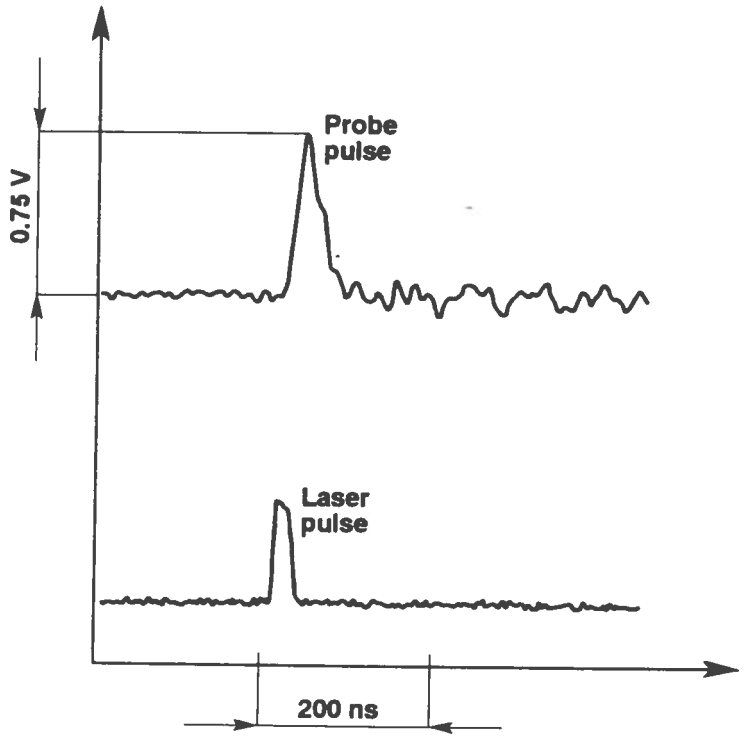

Fig. 8 – Waveforms of the KrCl laser pulse and of the Langmuir probe pulse. This last was recorded at 2mm from cathode.

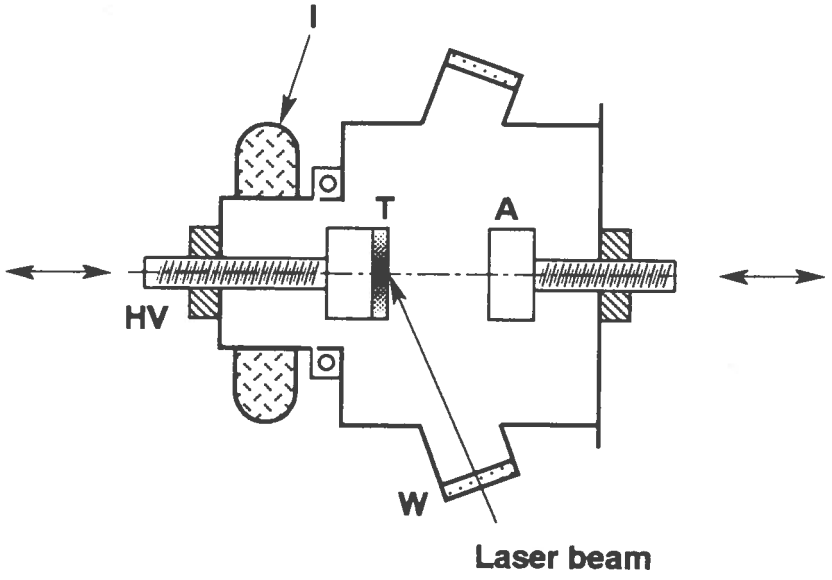

Fig. 9 – Accelerating chamber with a movable anode. T: Target, A: movable anode.

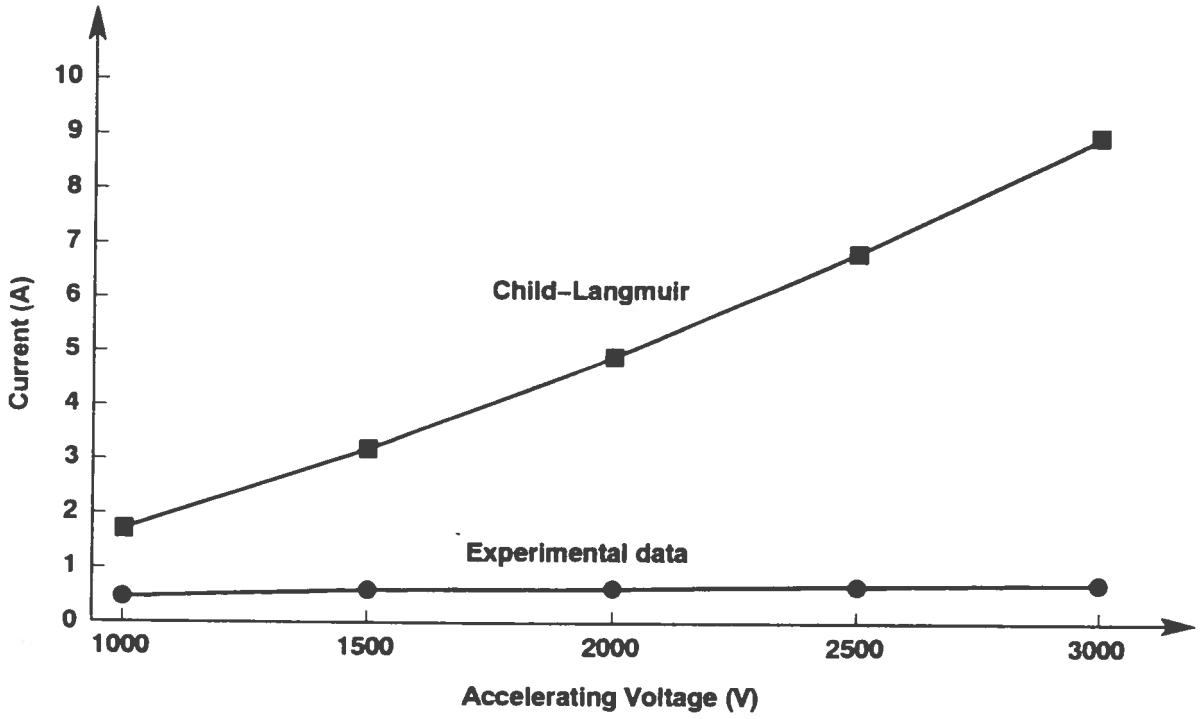

Fig. 10 – Experimental and theoretical current corresponding at a laser spot of 90 mm^2 and an anode-cathode distance of 2 mm.

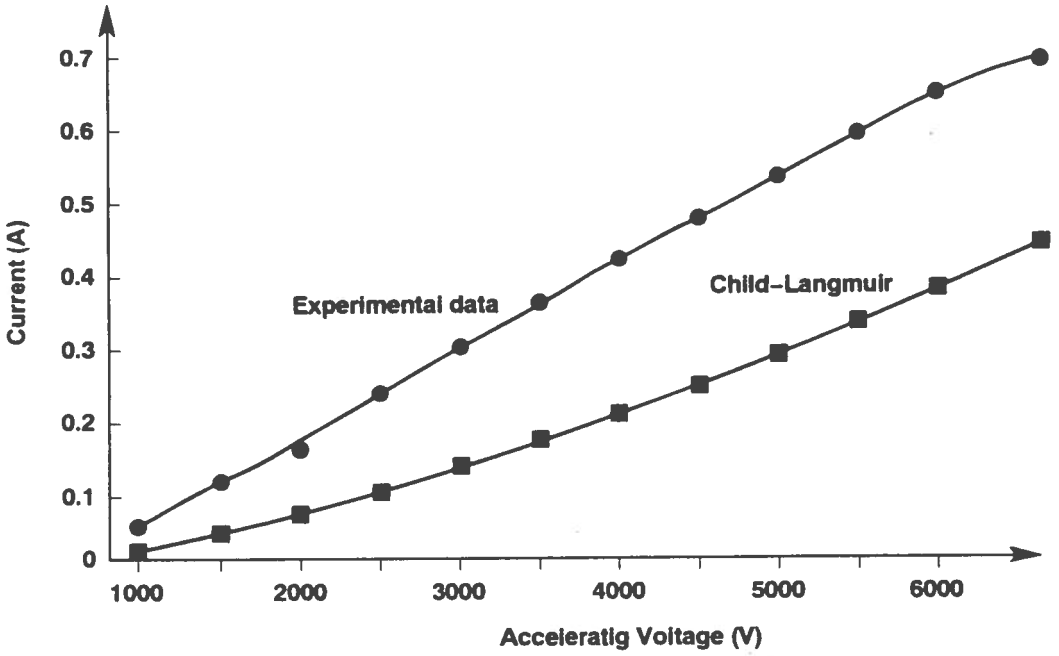

Fig. 11 – Experimental and theoretical current corresponding at a laser spot of 90 mm^2 and an anode-cathode distance of 16 mm.

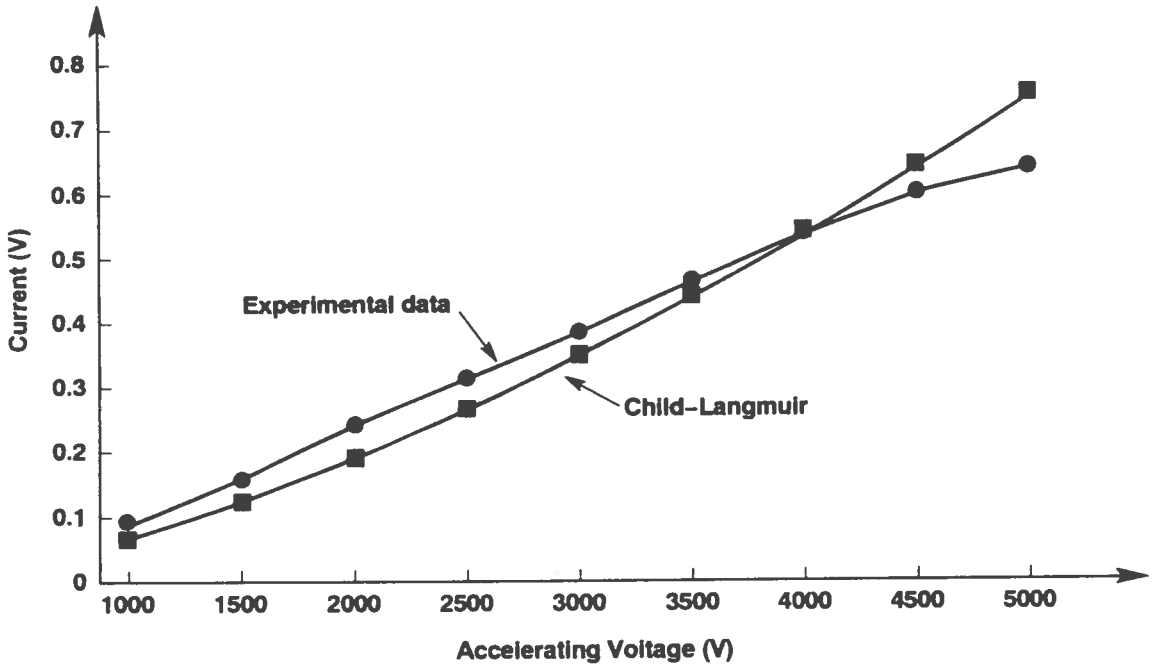

Fig. 12 – Experimental and theoretical current corresponding at a laser spot of 90 mm^2 and an anode-cathode distance of 10 mm.